Pharm Res (2016) 33:1998–2009
DOI 10.1007/s11095-016-1936-y

RESEARCH PAPER

Saquinavir Loaded Acetalated Dextran Microconfetti – a Long Acting Protease Inhibitor Injectable

Michael A. Collier[1] • Matthew D. Gallovic[2] • Eric M. Bachelder[1] • Craig D. Sykes[3] • Angela Kashuba[3] • Kristy M. Ainslie[1]

Received: 9 February 2016 / Accepted: 27 April 2016 / Published online: 6 May 2016

ABSTRACT

Purpose Since the adoption of highly active antiretroviral therapy, HIV disease progression has slowed across the world; however, patients are often required to take multiple medications daily of poorly bioavailable drugs via the oral route, leading to gastrointestinal irritation. Recently, long acting antiretroviral injectables that deliver drug for months at a time have moved into late phase clinical trials. Unfortunately, these solid phase crystal formulations have inherent drawbacks in potential dose dumping and a greater likelihood for burst release of drug compared to polymeric formulations.

Methods Using electrospinning, acetalated dextran scaffolds containing the protease inhibitor saquinavir were created. Grinding techniques were then used to process these scaffolds into injectables which are termed saquinavir microconfetti. Microconfetti was analyzed for *in vitro* and *in vivo* release kinetics.

Results Highly saquinavir loaded acetalated dextran electrospun fibers were able to be formed and processed into saquinavir microconfetti while other polymers such as poly lactic-co-glycolic acid and polycaprolactone were unable to do so. Saquinavir microconfetti release kinetics were able to be tuned via drug loading and polymer degradation rates. *In vivo*, a single subcutaneous injection of saquinavir microconfetti released drug for greater than a week with large tissue retention.

Conclusions Microconfetti is a uniquely tunable long acting injectable that would reduce the formation of adherence related HIV resistance. Our findings suggest that the injectable microconfetti delivery system could be used for long acting controlled release of saquinavir and other hydrophobic small molecule drugs.

KEY WORDS Biodegradable polymers · Drug delivery · Electrospinning · Microconfetti

ABBREVIATIONS

Ace-DEX	Acetalated dextran
FDA	Food and drug administration
GI tract	Gastrointestinal tract
HAART	Highly active antiretroviral therapy
HIV	Human immunodeficiency virus
MTB	*Mycobacterium tuberculosis*
PCL	Polycaprolactone
Pgp	P-glycoprotein
PIs	Protease inhibitors
PLGA	Poly lactic-co-glycolic acid
RTV	Ritonavir
SQV	Saquinavir
SQV-MC	Saquinavir microconfetti
WHO	World health organization

INTRODUCTION

According to the World Health Organization (WHO), over 35 million people worldwide are living with human immunodeficiency virus (HIV). Although HIV infection rates have

Electronic supplementary material The online version of this article (doi:10.1007/s11095-016-1936-y) contains supplementary material, which is available to authorized users.

✉ Kristy M. Ainslie
ainsliek@email.unc.edu

[1] Present address: Division of Molecular Pharmaceutics, Eshelman College of Pharmacy, University of North Carolina, 4211 Marsico Hall, 125 Mason Farm Road, Chapel Hill, North Carolina 27599, USA

[2] William G. Lowrie Department of Chemical and Biomolecular Engineering, College of Engineering, The Ohio State University, Columbus, Ohio 43210, USA

[3] Division of Experimental Therapeutics, Eshelman College of Pharmacy, University of North Carolina, Chapel Hill, North Carolina 27599, USA

slowed in recent years, the total number of people living with HIV has continued to rise (1). The first Food and Drug Administration (FDA) approved drug to treat HIV, azidothymidine, became available in 1987 and since then over 30 other drugs have been approved (2). These HIV drugs fall under five classes: Nucleoside/Nucleotide Reverse Transcriptase Inhibitors, Non-NRTIs, Protease Inhibitors (PIs), Entry/Fusion Inhibitors, and Integrase Inhibitors (2). Unfortunately, singular drug therapy is insufficient for effective HIV treatment, and thus, highly active antiretroviral therapy (HAART) consisting of multiple drug classes is required, every day for the rest of the patient's life. Since the introduction of these therapies, there has been a dramatic reduction in mortality and morbidity allowing patients to live longer and healthier lives (3); however, HAART treatment can still be rendered ineffective by the development of drug resistance (4).

The formation of drug resistant HIV is usually a result of mutations within the HIV genome that occurs during a period of inadequate drug exposure, typically caused from poor adherence to the prescribed drug regimen (5). A recent study looking at HAART adherence showed that only 55% of adults in North America and 77% of adults in Sub-Saharan Africa reached adequate adherence rates (6). Adherence rates of 95% or higher are required for successful treatments with singular PI-based combination therapy, which are difficult to achieve (5). Due to the turnover rate of HIV within infected patients, mutations that confer any selective advantage, such as a reduction in susceptibility to antiretroviral therapies, will result in a virus that proliferates at an alarming rate (7). While undergoing HAART, the chances of resistance formation are significantly decreased due to the multifaceted targets of the therapy; however, if resistance does occur during HAART, drug therapy options become limited. Unfortunately, the CDC claims that around 20% of patients in the United States undergoing HAART do not have suppression of viral loads suggesting either drug resistance or lack of adherence (8).

Drug combinations such as the PI saquinavir (SQV) boosted with ritonavir (RTV) (9) have slightly increased patient adherence rates for effective treatment. Twice daily boosted SQV was shown to produce better adherence related pharmacokinetic profiles which allows for more "forgiveness" when adherence is not 100% as higher trough concentrations of SQV are maintained for longer periods of time (10). RTV works by inhibiting p-glycoprotein (Pgp) efflux pumps and cytochrome P450 3A4 to allow for larger bioavailability and a longer SQV serum half-life; however, due to SQVs hydrophobic nature, its gastrointestinal tract (GI tract) absorption following oral administration is still undesirable (6).

One method to increase patient compliance and thus adherence rates is to use long acting injectables. Long acting injectables have been used for psychiatric disorders (11), contraception (12) and male hypogonadism (13) to increase compliance and allow for a subsequent reduction in time of inadequate drug exposure. Additionally, a subcutaneous or intramuscular injectable depot has the benefit of bypassing first pass metabolism, thus increasing drug bioavailability. This increase in drug bioavailability can drastically reduce the amount of drug required compared to an orally administered formulation (14). Furthermore, bypassing the GI tract is of importance as GI tract related adverse events are among the most common toxicities (15) reported with HAART that lead to regimen discontinuation (16, 17). Avoiding the GI tract discomfort associated with orally administered HAART could lead to better adherence rates from patients, which would reduce the chance of HIV resistant strain cultivation. Recently, TMC278 and GSK1265744 have been investigated as long acting injectables using nanosuspensions to provide a month's worth of drug in a single dose (18). While these two formulations are practical from an injectable mass standpoint, they do have some undesirable characteristics. One such characteristic is the non-tunable release kinetics because the hydrophobic interactions between drug and surfactant determine the rate of drug release and cannot be altered unless the drug or surfactant are changed (19). While long-term release is the goal, nanosuspensions can release drug for up to 12 months so if any site related toxicity or drug-drug interactions occur, the only option is to surgically remove the depot from the tissue. Additionally, depot drug concentrations remain extremely high even after serum drug concentrations have dropped below detection limits meaning there is slow and incomplete nanosuspension dissolution (20). Finally, nanosuspensions are not viable options for a large portion of HIV positive individuals who live in Sub-Saharan Africa because they are typically unstable outside of the cold-chain leading to uncharacterized release rates (21). This is particularly troubling as roughly 70% of all HIV positive individuals live within sub-Saharan Africa according to the WHO (1).

To help create a more manageable system without some of the side-effects observed with nanosuspensions, we applied a biodegradable polymer known as acetalated dextran (Ace-DEX) that can overcome the need for cold-chain storage. We have demonstrated that protein encapsulation within Ace-DEX alleviated the need for cold chain storage, and maintained protein bioactivity at elevated temperatures (22). Ace-DEX is derived from FDA-approved dextran and is made hydrophobic by forming acetal groups in place of hydroxyl groups along the glucose rings of the parent dextran molecules. Short reaction times create a larger percentage of acyclic acetals, which are the kinetically favorable product of the reaction. Extending the reaction time increases the amount of cyclic acetals, which resist hydrolytic cleavage better than acyclic acetals, allowing for more sustained polymer degradation in aqueous environments (23, 24). By shifting the reaction time, we can effectively tune the degradation rate of polymer constructs from days to weeks in

pH-neutral extracellular conditions (23). Our group has used electrospun Ace-DEX scaffolds for temporal release of therapeutics to be used as a topical, or surgically implantable long acting release vehicle (25). Since that work, our group has become interested in taking advantage of Ace-DEX's high glass transition temperature (~160–190°C) (22) to process these long fibers into smaller injectable constructs. Polyesters such as poly lactic-co-glycolic acid (PLGA), polycaprolactone (PCL) and poly lactic acid (PLA) are typically used for electrospinning (26), however, their glass transition temperature is around 50°C and limits their ability to be processed post spinning (27, 28). Here we present electrospun Ace-DEX scaffolds, unlike PCL and PLGA scaffolds, can be successfully processed into dispersible, high drug content injectables (termed Ace-DEX microconfetti (Ace-DEX-MC)) for long acting release. In this manuscript, we show that Ace-DEX scaffolds containing SQV at high loadings can be turned into MC. Saquinavir microconfetti (SQV-MC) can release drug at variable rates according to polymer degradability and loading, and release drug *in vivo* for more than a week from a single injection.

MATERIALS AND METHODS

A majority of the materials were purchased from Sigma Aldrich (St. Louis, MO, USA) and used without further modifications. Saquinavir was purchased from Proactive Molecular Research (Alachua, FL, USA). Water was purified using a Millipore Milli-Q integral water purification system (Billerica, MA, USA).

Ace-DEX Synthesis from 71 and 500 kDa Dextran

Ace-DEX polymer was synthesized using 71 or 500 kDa dextran from *Leuconostoc mesenteroides* with some modifications to the previously described protocol. (23) To synthesize 71 kDa Ace-DEX, lyophilized 71 kDa dextran (1.0 g) and pyridinium p-toluenesulfonate (0.0617 mmol) were dissolved in 10 mL of anhydrous dimethyl sulfoxide (DMSO). To synthesize 500 kDa Ace-DEX, lyophilized 500 kDa dextran (0.5 g) and pyridinium p-toluenesulfonate (0.0308 mmol) were dissolved in 8 mL of DMSO. Dissolved dextrans were reacted with Waterstone 2-ethoxypropene (Carmel, IN, USA) under nitrogen gas at room temperature for the desired duration to achieve 37 or 52% relative cyclic acetal coverage, which we will refer to as fast and slow degrading Ace-DEX, respectively. After the desired length of reaction, reactions were quenched with an excess of trimethylamine (TEA). While the acetalation process will result in increased molecular weights greater than 71 and 500 kDa, we will still refer to them as 71 and 500 kDa Ace-DEX in this work. The reaction volumes were then precipitated in basic water (.04/99.96% v/v TEA and Water respectively), and centrifuged at 14,500 rpm for 10 min at 4°C using a Thermo Scientific sorvall legend XTR centrifuge (Waltham, MA, USA) to remove any remaining water-soluble polysaccharides (i.e., un-acetalated dextran and/or lowly acetalated dextran). The resulting pellet was then frozen and lyophilized overnight. To further purify the polymer, the product was dissolved in ethanol and centrifuged at 14,500 RPM for 10 min at 4°C the following day. The supernatant was precipitated in basic water, centrifuged again, frozen and lyophilized to yield 71 or 500 kDa Ace-DEX polymer. The extent of cyclic acetal formation was determined using ^{1}H nuclear magnetic resonance (NMR) spectroscopy based on a previously developed method (23).

Optimization of 71 and 500 kDa Ace-DEX Electrospinning

Ace-DEX scaffolds were first generated by dissolving 71 or 500 kDa Ace-DEX at various concentrations in a hexafluoroisopropanol (HFIP), n-butanol, and TEA solution (59.5/39.5/1.0% v/v/v). When fully dissolved, the solution was loaded into a Hamilton gaslight glass model 1001 syringe (Reno, NV, USA) and a Hamilton metal hub blunt point needle (Reno, NV, USA) was attached. When fully primed, the syringe was loaded onto an Analytical West Inc. scientific lab supply syringe pump (Lebanon, PA, USA). The syringe needle was connected to a positive voltage and a flat sheet of aluminum foil was connected to a negative voltage on a Gamma High Voltage Research power supply (Ormond Beach, FL, USA). When flow was initiated at 1 mL/hr from the syringe pump, a voltage difference of roughly 15 kV was used to break the surface tension of the droplet and force the droplet into a Taylor cone. Following scaffold collection, small representative samples were adhered to Ted Pella aluminum specimen mounts (Redding, CA, USA) using carbon tape. Images were acquired using either an FEI NOVA NanoSEM 400 located at The Ohio State University, or a Hitachi S-4700 Cold Cathode Field Emission Scanning Electron Microscope located at the University of North Carolina.

Production of Ace-DEX, PLGA and PCL Microconfetti

Scaffold production of either 71 or 500 kDa Ace-DEX was performed at the optimal electrospinning concentration as described above. Ace-DEX scaffolds were removed from the aluminum foil sheet and transferred to a Kyocera CM-10 BK ceramic grinder (Costa Mesa, CA, USA) for processing into microconfetti (MC). Additional Ace-DEX scaffold samples were transferred to a Retsh 10 mL stainless steel grinder jar (Newton, PA, USA) that had been cooled in liquid nitrogen for 10 min. The loaded stainless steel grinder jar was then placed into a Glen Mills high speed mixer mill (Clifton, NJ,

USA) and run for 5 min at 10 Hz for processing into MC. Other Ace-DEX scaffold samples were sent to Retsch (Newton, PA, USA) to be processed into MC using a cryomill (5 min precool, 5 min at 15 Hz). All MC samples were imaged using SEM as described above.

50:50 PLGA (50–70 kDa) was dissolved in a solution of HFIP and n-butanol (80/20% v/v), loaded into a syringe and electrospun onto aluminum foil at 1 mL/hr using a voltage difference of 20 kV. PLGA scaffolds could not be processed using the ceramic grinder. Additional PLGA scaffold samples were transferred to a stainless steel grinder jar that had been cooled in liquid nitrogen for 10 min. The high speed mixer mill was run for 5 min at 10 Hz. Following high speed mixer milling, the sample was removed and imaged using SEM.

PCL (70–90 kDa) was dissolved in pure chloroform, loaded into a syringe and electrospun onto aluminum foil at 3 mL/hr using a voltage difference of 20 kV. PCL scaffolds could not be processed using the ceramic grinder nor high speed mixer mill. Scaffold samples were sent to Retsch to be processed using a cryomill. Following cryomilling, samples were imaged using SEM.

Production of Saquinavir Loaded 71 and 500 kDa Ace-DEX Microconfetti

Ace-DEX scaffolds were generated by dissolving 71 or 500 kDa Ace-DEX (400 or 200 mg/mL, respectively) with the desired amount of SQV (10, 20, 30, 40 or 50% wt/wt) in a solution of HFIP, n-butanol and TEA (59.5/39.5/1.0% v/v/v). The SQV Ace-DEX scaffold was then allowed to dry under N_2 gas for 5 min to ensure all solvents had evaporated. The scaffold was then processed using the ceramic grinder to yield SQV-MC and stored at -20°C until further use.

Encapsulation Efficiencies of SQV-MC

Following generation of Ace-DEX SQV-MC, encapsulation efficiencies were determined by preparing a 1 mg/mL solution of SQV-MC dissolved in high performance liquid chromatography (HPLC) grade methanol and MilliQ water (80/20% v/v). These samples were analyzed using an Agilent Technologies Series 1100 HPLC (Santa Clara, CA, USA) with an Agilent Eclipse Plus C18 column (4.6 × 150 mm) at a flow rate of 1 mL/min, injection volume of 60 μL and a detection wavelength of 240 nm alongside a standard curve of un-encapsulated SQV. The drug elution time was ~6 min, and following the HPLC run, the amount of encapsulated SQV was determined.

SQV-MC *In Vitro* Release Curves

Briefly, 71 and 500 kDa SQV-MC samples were suspended at a concentration of 2 mg/mL with 0.01% v/v Tween 80 (specific gravity = 1.06) in phosphate-buffered saline (PBS) at pH 7.4. Once in suspension, varying quantities, dependent on SQV loadings, were placed into Thermo Fisher Scientific snakeskin dialysis bags with an 8 kDa cutoff, (Grand Island, NY, USA). The dialysis bags ($n = 3$ per time point), were placed into 1 L beakers with PBS on a Thermo Fisher Scientific RT2 advanced hotplate (Grand Island, NY, USA) set to 37°C. As the drug released from the SQV-MC, it passed through the dialysis membrane into the PBS sink. At each time point, individual dialysis bags were removed from the beaker and 200 mL of PBS sink was emptied to keep a constant dialysis bag to PBS volume ratio. Residual SQV-MC was removed from the dialysis bag by washing with excess basic water. This was then centrifuged at 4,000 RPM for 10 min at 4°C to pellet any residual SQV-MC. The supernatant was removed, and the pelleted SQV-MC was frozen and lyophilized. At the final time point, one additional sample was suspended in 0.01% v/v Tween 80 in PBS (pH 7.4), placed in a dialysis bag and then removed like every other sample. This specimen represented a "0 h" time point release. Following sample lyophilization, all samples were dissolved in 3 mL of HPLC-grade methanol and Milli-Q water (80/20% v/v) and analyzed using the HPLC method outlined for encapsulation efficiency. Percent SQV release was then calculated relative to the "0 h" data point.

In Vivo Release of SQV-MC

ICR mice (female, 8–10 weeks old) were purchased from Taconic Farms (Hudson, NY, USA). The two groups consisted of 71 kDa fast degrading 10 and 30% SQV-MC. 8 mg of each SQV-MC (266 mg/kg of polymer) was injected equating to roughly 26.6 and 80 mg/kg of SQV, respectively. SQV-MC was suspended in 0.01% v/v Tween 80 in PBS (pH 7.4), mice were placed under light anesthesia using isoflurane, and 300 μL was injected into the subcutaneous space (left flank). Collection time points were 20 min, 1, 3 and 7 days post injection. At each time point, mice ($n = 2$) were euthanized in a CO_2 chamber followed by cardiac puncture to collect blood. Serum was then obtained by centrifuging the blood samples in Becton Dickinson microtainer heparin lined tubes (Franklin Lakes, NJ, USA) for 5 min in a VWR mini centrifuge (Radnor, PA, USA) and freezing it on dry ice. The spleen, liver, kidney and brain were also harvested and rapidly frozen in liquid nitrogen. All samples were then stored at -80°C until quantification.

LC/MS Quantification of Serum and Tissue Samples

Following extraction from the mice, serum and tissue samples were analyzed for SQV content based on previously published work (29). The quantity of SQV in samples was determined

using Sciex Analyst Chromatography Software on a Sciex API-5000 triple quadrupole (Foster City, CA, USA) Liquid Chromatography Mass Spectrometry (LC/MS) machine. Calibration curves were obtained by using a weighted linear regression of analyte:internal standard peak area ratio *vs.* concentration curve. The quantity of SQV within each sample was determined from this calibration curve.

RESULTS

Optimization of 71 and 500 kDa Ace-DEX Electrospinning

Ace-DEX scaffolds were created by electrospinning 71 and 500 kDa Ace-DEX using an HFIP, n-butanol and TEA solution. Concentrations well below the optimal spinning concentration of 200 and 400 mg/mL for 71 and 500 kDa, respectively, led to more erratic Taylor cone stability and yielded pseudo fiber-particle combinations (Fig. 1a and d). At concentrations closer to the optimal spinning concentration, undesirable spindly fibers with fewer intermittent particles were observed (Fig. 1b and e). At optimal spinning concentrations of 400 and 200 mg/mL for 71 and 500 kDa Ace-DEX, respectively, homogenous ribbon-like fibers were seen (Fig. 1c and f).

Production of Ace-DEX, PLGA and PCL Scaffold Microconfetti

Ace-DEX scaffolds had a fluffy texture and were easily removed from aluminum foil whereas PLGA and PCL scaffolds were more rigid and more difficult to collect. Processed PLGA (high speed mix mill) and PCL (cryomill) scaffolds were completely fused (Fig. 2a and b). The fused PLGA made collection from the jar difficult even after cooling the high speed mixer jar in liquid nitrogen. Cryomilled PCL formed small powdery aggregates without well-defined structures. Ace-DEX-MC generated by high speed mixer milling and cryomilling were a fine powder of small fractured fibers of relatively polydisperse size (Fig. 2c and d). The ribbon fiber morphology was retained throughout the grinding process and minimal, if any, fusion was seen. Ace-DEX-MC generated with the ceramic grinder was a fine powder of large fractured fibers of relatively polydisperse size (Fig. 2e and f). The ribbon fiber morphology was retained throughout the grinding process and minimal, if any, fusion was observed.

Encapsulation Efficiencies of SQV-MC

Due to the large quantities of SQV required, care was taken to ensure all solids were in complete solution before proceeding to electrospinning. All Ace-DEX SQV-MC was loaded at extremely high efficiency with the lowest encapsulation efficiency being 98.2% (Table I). The consistent drug loading (from initial to final) demonstrates this.

71kDa SQV-MC *In Vitro* Release Curves

In vitro release profiles were generated to determine the release kinetics of SQV-MC depending on SQV weight loading and Ace-DEX polymer degradation rate (Fig. 3a, b, c and d). All samples exhibited a burst release of SQV within the first 2 h followed by relatively linear release afterwards. As drug loading in fast degrading Ace-DEX-MC increased, so too did burst release of SQV. With slower degrading Ace-DEX, however, there was no clear trend as burst release values remained fairly consistent across SQV loadings. Throughout all samples, it was seen that increasing the drug loading increased

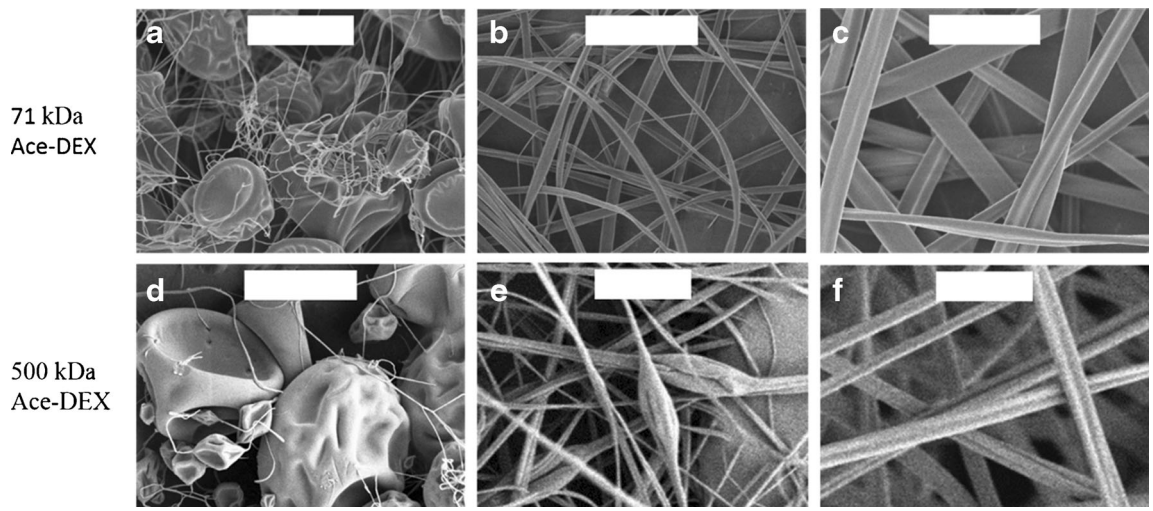

Fig. 1 Scanning electron micrographs with scale bar indicating 5 μm for electrospun constructs fabricated from 71 kDa acetalated dextran (Ace-DEX) at a concentration of (**a**) 200 mg/mL, (**b**) 300 mg/mL and (**c**) 400 mg/mL, and 500 kDa Ace-DEX at a concentration of (**d**) 100 mg/mL, (**e**) 150 mg/mL and (**f**) 200 mg/mL.

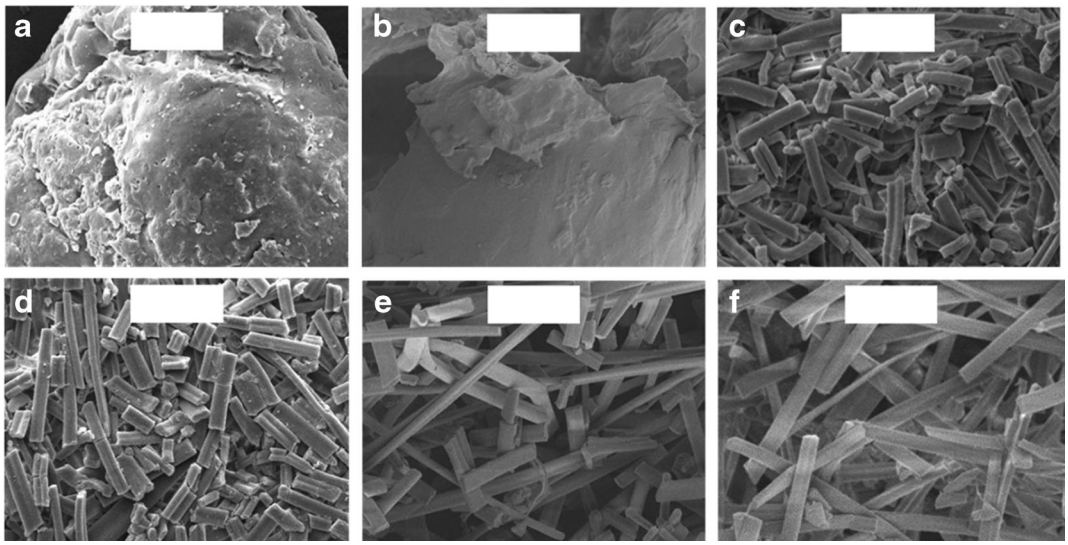

Fig. 2 Scanning electron micrographs with scale bar indicating 10 μm of (**a**) poly lactic glycolic acid (PLGA), (**b**) polycaprolactone (PCL), (**c**–**e**) 71 kDa acetalated dextran (Ace-DEX) and (**f**) 500 kDa Ace-DEX scaffolds processed by (**a**, **c**) high speed mixer milling, (**b**, **d**) cryomilling or e, (**f**) ceramic grinding.

the release of SQV at 24 h. In fact, with the 40% SQV-MC, there was greater than 50% SQV release within the first 24 h. Throughout all samples, the slower degrading Ace-DEX showed a more sustained release of SQV even when increasing the SQV loading.

500kDa SQV-MC *In Vitro* Release Curves

In vitro release profiles were generated from the higher molecular weight SQV-MC to determine if higher loading could be achieved with similar release patterns (Fig. 4). Both the slow and fast degrading Ace-DEX exhibited a burst release of SQV within the first 2 h followed by relatively linear release afterwards. Similar to the 71 kDa SQV-MC, an increase in the cyclic acetal coverage led to a reduction in the degradation rate of Ace-DEX and a more sustained release. Interestingly, the 50% 500 kDa SQV-MC released SQV at a slower rate than the 40% 71 kDa SQV-MC using both the fast and slow degrading Ace-DEX polymers.

In Vivo Release

Serum concentration-time profiles were generated by taking time points at 20 min, 1, 3 and 7 days post injection (Fig. 5). 20 min' post-injection demonstrated a large burst release of SQV into the serum for both groups (67.45 and 144.5 ng/mL for 10 and 30% SQV-MC, respectively). Following the initial burst of SQV, there was a fairly linear release of SQV into the serum for both the 10 and 30% SQV-MC injection groups. However, on day 7, the 10% SQV-MC injection exhibited a spike in serum concentration which boosted the serum concentration to 32.9 ng/mL.

Tissue SQV concentrations were analyzed from the 30% SQV-MC injection group at 20 min, 1, 3 and 7 days post-injection (Fig. 6). There was not any detectable SQV within the brain at any time point. Twenty minutes after injection, there was SQV within both the kidneys and liver (42.6 and 33.8 ng/mg respectively), however, SQV was undetectable within the spleen. SQV concentrations remained fairly stable within the liver over the duration of the 7 day study. One day

Table I Initial Weight Loading, Encapsulation Efficiency, Final Weight Loading and *In Vitro* Release Half-Lives of Saquinavir (SQV) at pH 7.4 for SQV Loaded Microconfetti Composed of 71 and 500 kDa Acetalated Dextran (Ace-DEX) Polymer with Either Fast or Slow Degrading Properties (37 and 52% Cyclic Acetal Coverage, Respectively)

Microconfetti Polymer	Initial Loading [wt.%]	Encapsulation Efficiency [%]	Final Loading Fast Degrading Polymer [wt.%]	Half-lives [hr]	Encapsulation Efficiency [%]	Final Loading Slow Degrading polymer [wt.%]	Half-lives [hr]
71 kDa Ace-DEX	10	99.6 ± 3.4	9.96 ± 0.30	65.26	101 ± 2.4	10.1 ± 0.24	271.10
	20	100.2 ± 2.5	20.0 ± 0.50	60.33	101.8 ± 2.1	20.4 ± 0.40	172.60
	30	100.1 ± 1.2	30.0 ± 0.40	51.25	98.7 ± 0.9	29.6 ± 0.26	156.50
	40	100.0 ± 2.7	40.0 ± 1.06	13.68	101.0 ± 1.1	40.4 ± 0.50	137.20
500 kDa Ace-DEX	50	98.9 ± 1.8	49.5 ± 0.90	15.65	98.2 ± 0.8	49.1 ± 0.40	152.60

Data are presented as mean ± standard deviation ($n = 3$)

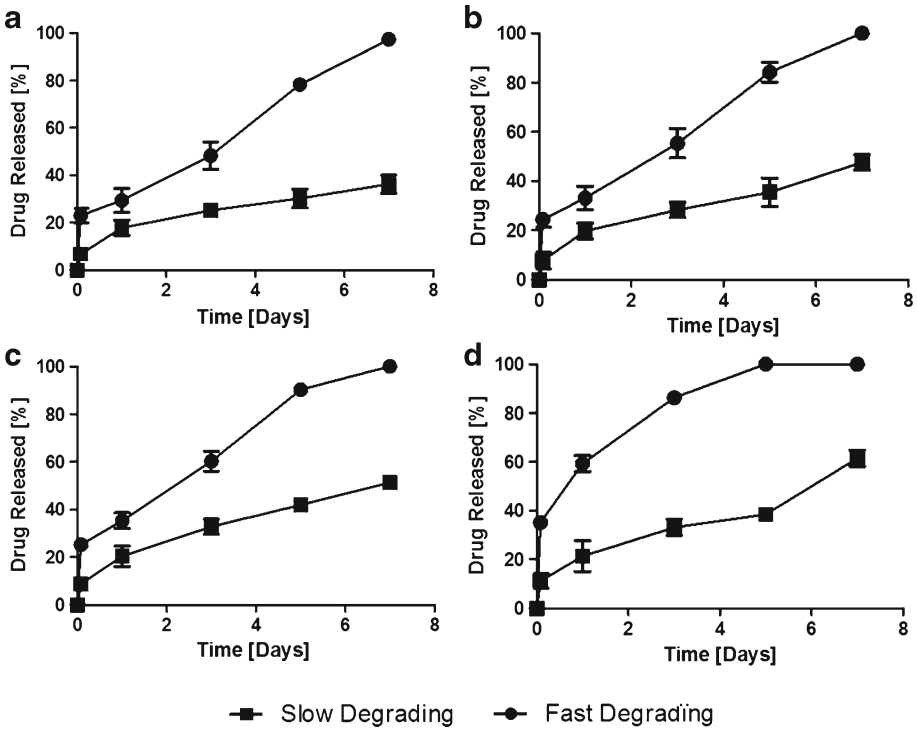

Fig. 3 *In vitro* saquinavir release profiles performed at pH 7.4 for drug loaded microconfetti composed of fast or slow degrading (37 and 52% cyclic acetal coverage, respectively) 71 kDa acetalated dextran with different drug weight loadings: (**a**) 10%, (**b**) 20%, (**c**) 30% and d) 40%. Data are presented as mean ± standard deviation ($n = 3$).

after injection, accumulation within the kidneys and spleen drastically increased (315.4 and 179.3 ng/mg, respectively). Following the high concentration within the kidney and spleen on day 1, the concentrations dropped slightly 3 days post injection and concentrations approached baseline levels 7 days post injection.

DISCUSSION

It has been reported that upwards of 20% of HIV positive patients within the United States are infected with strains that confer at least partial resistance to one or more available treatments with increases of more than 5% annually for at least one class of HIV therapies (30). The lack of adherence to HAART within the infected community could mirror the complications faced with treatments against other resistant pathogens (e.g., *Staphylococcus aureus* (31) and *Mycobacterium tuberculosis* (MTB) (32)). Long acting drug delivery systems have the ability to overcome the resistance complications associated with non-adherence as they enable fewer administrations within the dosing regimen. Here we use the novel, highly loaded and tunable injectable release system of Ace-DEX-MC for the sustained delivery of SQV.

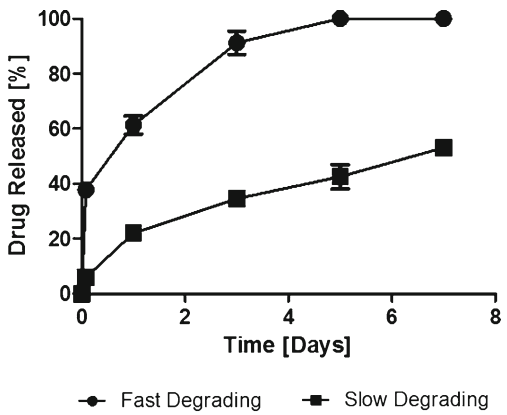

Fig. 4 *In vitro* saquinavir release profiles performed at pH 7.4 for microconfetti with a drug weight loading of 50%, composed of fast or slow degrading (37 and 52% cyclic acetal coverage, respectively) 500 kDa acetalated dextran. Data are presented as mean ± standard deviation ($n = 3$).

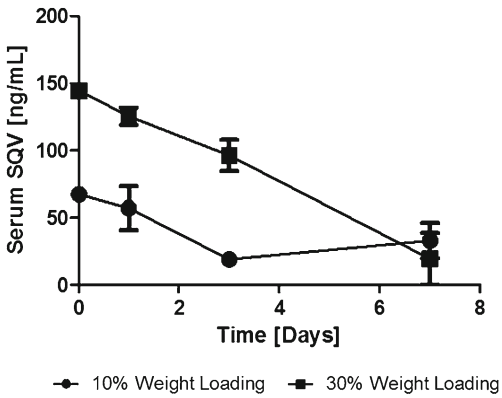

Fig. 5 Serum concentrations of saquinavir (SQV) following *in vivo* release from fast degrading (37% cyclic acetal coverage) 71 kDa acetalated dextran microconfetti loaded with 10 and 30% SQV by weight. Data are presented as mean ± standard deviation ($n = 2$).

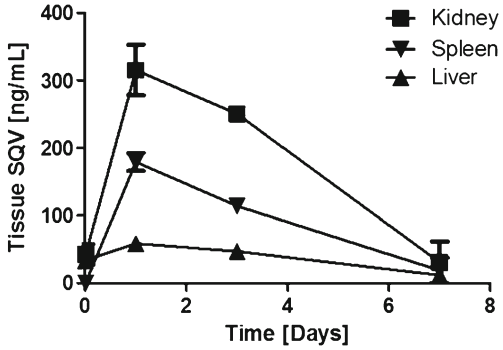

Fig. 6 Tissue concentrations of saquinavir (SQV) following *in vivo* release from fast degrading (37% cyclic acetal coverage) 71 kDa acetalated dextran microconfetti loaded with 30% SQV by weight. Data are presented as mean ± standard deviation ($n = 2$).

We were able to electrospin homogenous ribbon-like fibers of both 71 and 500 kDa Ace-DEX scaffolds by increasing the concentration of polymer within the solvent system to 400 and 200 mg/mL, respectively, as seen in Fig. 1. The ribbon morphology observed here is due to the highly volatile solvent system which evaporates quickly causing a polymer fiber shell to collapse on itself. (33) During the electrospinning process, the polymer, drug and solvent system travel through the air to a grounded plate. As they travel, the solvent system evaporates leaving the polymer to harden into fibers containing the drug. Due to the fact that there is no external liquid continuous phase, such as the water that is commonly used in emulsion particle formulations (34), drug remains within the fibers which leads to the high encapsulation efficiencies (Table I). Furthermore, it has been reported that when a drug is not readily soluble within the electrospinning solution, drug crystals are visible within the fibers and lead to a substantial burst release of drug even at low drug loadings (35). Considering SQV has relatively good solubility within our solvent system, this is not an issue and drug crystals are not seen on the fibers (Supplemental Fig. 1).

Due to electrospun scaffolds' ability to encapsulate drug at high loadings, they are desirable for extended drug delivery. Highly loaded polymeric scaffolds have been used to treat stenosis through surgical implantation (36); however, this is highly unfavorable and impractical for frequent (e.g., weekly or bi-weekly) treatments. Long acting injectables such as Risperdal® Consta® microparticles can have encapsulation efficiencies as low as 20%, which wastes a large quantity of drug (37). This can be further problematic for drugs that are not very potent, as these low encapsulation efficiencies lead to final weight loadings of ~12–15% which require extremely high polymer doses for any given treatment. For example, SQV requires 2 g or greater for daily oral dosing (4% bioavailability without RTV), so a long acting injectable for weekly doses at loading similar to Risperdal® Consta® could require greater than 5 g of polymer, when currently the maximum amount of polymer in an injectable is 1.2 g for Vivitrol® (38). One of the hallmarks of the injectable nanosuspensions TMC278 and GSK1265744 is that the drug content is ~80% by weight and the drugs themselves are extremely potent allowing for minimal excipient load (18). However, the cold chain storage requirements significantly limit the usage of these treatments within the developing world, especially within sub-Saharan Africa where cold chain storage is not readily available (39). As previously mentioned, Ace-DEX has the ability to maintain cargo stability at elevated temperatures alleviating cold chain requirements that are often needed for other biopolymers such as PLGA (22), which further strengthens the wide applicability of SQV-MC. Future studies will analyze SQV-MC release kinetics and bioactivity after storage at elevated temperatures.

SQV is known to be more effective within T cells than within macrophages suggesting that SQV can be readily oxidized in oxidative environments, diminishing its activity (40). While the activity of SQV has not been affected by incubation with H_2O_2 (41), SQV is highly oxidized via cytochrome P450 3A4 (42) and thus there exists the possibility of losing efficacy when stored in oxygen rich environments. Future studies will determine if encapsulation within MC has the ability to protect SQV from oxidation and preserve activity.

Because polymer scaffolds require surgical implantation and current FDA-approved long-acting formulations have manufacturing and storage concerns, we designed a system where highly loaded Ace-DEX scaffolds can be processed into an injectable formulation called MC. As mentioned previously, Ace-DEX has a glass transition temperature of roughly 160–190°C (22) while PLGA and PCL are closer to 50°C (27, 28). When PLGA or PCL scaffolds are processed using a high speed mixer mill or cryomill, respectively, the MC from these polymers fuse to form large aggregates (Fig. 2). This occurs because a significant amount of local heat is generated when the ball impacts the jar (43). As the heat transfers into the PCL and PLGA materials, the temperature rises above their glass transition and changes their physical structure from rigid to amorphous which causes fusion. We have previously shown that microparticulate Ace-DEX can resist agglomeration at elevated temperatures while PLGA microparticles do not (22). Slight agglomeration of Ace-DEX fibers was accomplished by grinding scaffolds with a mortar and pestle as shown in Supplemental Fig. 2; however, this technique was not used any further. Ace-DEX has the capability to be processed into MC of different sizes depending on the energy of the grinding procedure as seen within Fig. 2. When we used the high speed mixer mill and cryomill (high energy processes), smaller MC fragments were created which could be used for intracellular delivery of therapeutics as these MC fragments would be readily engulfed by phagocytes, similarly to the elliptical disks used by Champion et al. (44). The ceramic grinder created larger fragments which are advantageous for sustained delivery to systemic circulation, as objects

larger than 10 μm in length will effectively evade phagocytic uptake (45). Future research will be performed to determine the degree at which ceramic grinder-processed MC resist phagocytosis. Since our goal is to actively deliver drug into systemic circulation over an extended period of time, we chose to investigate the use of larger MC generated by the ceramic grinder.

Another advantageous characteristic of Ace-DEX is its tunable hydrolytic degradation rates that are simply based on the synthesis reaction time and subsequent cyclic acetal coverage. Polysaccharides such as dextran, used for controlled drug delivery are noted to release cargo via diffusion and/or dissolution (46). As seen in Figs. 3 and 4, the rate of SQV release from SQV-MC can be increased by decreasing the cyclic acetal coverage, which subsequently increases the degradation rate of the polymer. Because SQV is a fairly hydrophobic drug with a log P value of ~ 1.9 (47), it will prefer to reside within the hydrophobic polymer matrix rather than diffusing into the aqueous environment. Upon hydrolysis, the fiber will begin to erode and SQV will be released. With the faster degrading Ace-DEX-MC, there is a substantial burst release followed by a less drastic sustained release from all loadings and polymer molecular weights. We believe this large burst release occurs because of a combination of drug located on the surface of the fibers, and the smaller number of cyclic acetals (larger number of acyclic acetals) leads to more extensive initial hydrolysis, allowing for rapid fiber dissolution. Alternatively, the slow degrading Ace-DEX has a drastically smaller burst release, likely due to the fact that far more of the acetal groups are cyclic acetals limiting the hydrolysis of the polymer within the first few hours in an aqueous solution and for the duration of release. While there is a small burst with the slower degrading Ace-DEX, this likely comes from the drug located on the surface of the MC. Due to the fact that SQV is released predominantly through polymer degradation/dissolution, complete drug release from implanted PLGA scaffolds could take weeks to months. In fact, Crow et al. have shown that drug release from PLGA fibers can have half-lives of greater than 9 weeks (48). The slow SQV release kinetics that PLGA would likely exhibit might lead to inadequate serum concentrations. Since PLGA cannot be processed into injectable MC, surgical implantation would be required, making PLGA very undesirable for this application.

There is a clear trend that with increased loading, the drug will release more quickly from both the fast and slow degrading Ace-DEX groups. This most likely stems from the fact that as the drug content within the fiber increases, the polymer matrix within the fiber becomes more unstable with reduced polymer entanglement that would restrict drug release. Interestingly, the 71 kDa 40% SQV-MC releases drug faster than even the 500 kDa 50% SQV-MC with both the fast and slow degrading Ace-DEX. We believe this occurs because at the weight loading of 40% with 71 kDa Ace-DEX, we are approaching the solubility limit of SQV in our solvent system when using a concentration of ~262 mg/mL. Indeed, the Taylor cone generated from these electrospinning conditions was less stable than the other samples, perhaps indicating that not all of the components were completely dissolved. When the molecular weight is increased to 500 kDa the solution becomes more viscous, allowing for a smaller polymer concentration required for stable Taylor cone formation, thus leading to a lower SQV concentration needed for fabrication (i.e., a weight loading of 50% using 500 kDa Ace-DEX has a SQV concentration of ~200 mg/mL in the solvent system).

To analyze the ability of SQV-MC to be used as a sustained delivery vehicle, we injected ICR mice subcutaneously with the fast degrading 71 kDa 10 and 30% SQV-MC. The fast degrading Ace-DEX was selected because mice are known to have faster systemic circulation clearance rates than humans (49) and slow releasing SQV-MC might not release drug fast enough for sufficient serum and tissue accumulation. In fact, the total systemic clearance of SQV is around 4.81 L/h/kg in mice (50) and 1.14 L/h/kg in humans (51). We injected 8 mg of each MC formulation which contained 0.8 and 2.4 mg SQV for 10 and 30% SQV-MC respectively. 8 mg of SQV-MC was selected because we believed it was more than likely that different masses of polymer would lead to differential degradation and release rates independent of the SQV loading. The subcutaneous administration route was selected considering Gautam et al. have shown that the subcutaneous space was satisfactory for release of antiretrovirals and enables a larger injection volume than does the intramuscular space (52).

For the 30% SQV-MC, a large burst was seen after injection resulting in high concentrations of SQV within the serum. This was not surprising as the polymer will begin degrading following introduction to an aqueous environment, and any surface SQV would likely be released instantaneously. Following the burst release from SQV-MC into the serum, the serum levels of SQV steadily decline as the clearance rate of SQV out of circulation was likely faster than the release rate of SQV from the MC. It is conceivable that high serum concentrations of SQV in humans could be achieved for much longer than they were in the ICR mice due to the drastic differences in typical SQV clearance rates in each species. The 10% SQV-MC saw a large burst almost instantaneously, similar to the burst seen with the 30% SQV-MC followed by a steady decline in serum SQV concentrations. Interestingly, there was an unexpected secondary burst of SQV from the injection depot following 3 days of release. We believe this secondary burst is the result of a sudden degradation of a pocket of SQV-MC within the depot. The secondary burst phenomenon has previously been reported when using PLGA microspheres for sustained release of a hydrophobic PI which suggests that it could possibly be related to drug cargo (53).

The concentration at which 90% of viral growth is inhibited (IC-90) for SQV is noted to be anywhere from 3 to 50 ng/mL in serum (51) which is reached during the majority of the 1 week timeframe with the 30% SQV-MC but not with the 10% SQV-MC. However, with a 4-fold lower clearance rate within humans, it is possible that concentrations above the IC-90 could be reached for a longer duration than was shown within this study. Future studies plan to use larger groups and use longer durations for release with SQV-MC.

When adhering to the proper HAART regimen, serum viremia can be controlled; however, HIV still has the ability to develop reservoir infection sites in the brain, spleen, gastrointestinal tract, lymphoid tissue and other organs in which there is differential drug distribution allowing for increased chances for resistance (54). We analyzed the tissue accumulation of SQV following release from the 30% SQV-MC in the same mice that had their serum samples analyzed. As can be observed in Fig. 6, there is an initial accumulation peak of SQV within the tissues following 1 day of release from SQV-MC followed by a steady drop in the tissue content of SQV until 7 days when there are very low levels of tissue SQV. SQV is not privy to crossing the blood brain barrier as has previously been reported (42), most likely due to high Pgp activity at the blood brain barrier interface. It was our initial hypothesis that constant release of SQV into circulation could potentially overwhelm the available Pgp pumps allowing for some accumulation, but that action was not achieved. PI's like SQV have recently been noted for inducing significant hepatotoxicity within HIV positive individuals (42). This may be explained by SQV predominantly being metabolized within the liver by cytochrome P-450 3A4 (55) as well as direct passage to the liver after oral delivery of conventional formulations. SQV accumulation within the liver of our mice was lower than the drug amounts in all organs other than the brain. Thereby, our formulation should reduce the concentration of SQV that reaches the liver, compared to current oral formulations. Future work will focus on determining if constant SQV release from SQV-MC leads to elevated aspartate aminotransferase levels, indicative of hepatotoxicity as well as how these levels compare to the oral formulation.

Before the HAART era, HIV patients displayed white-pulp depletion within their spleens (56), which signifies significant T-cell reduction, increasing the chances for opportunistic infections such as bacterial pneumonia, MTB and many others (2). Since the induction of HAART in the mid-1990s, life expectancy, quality of life and the risk of opportunistic infections have dramatically improved confounded with a conservation of white-pulp within HIV patient's spleens indicating the importance of the spleen within the HIV infection process (56). It has been reported that the spleen contains close to 15% of the total lymphocytes in the body (greater than any other organ) which are the primary targets of HIV (57). It is therefore significant that the spleen was able to accumulate a large quantity of the SQV released from SQV-MC as this is a likely reservoir organ for the virus, and as a number of antiretroviral drugs accumulate poorly within the spleen (57).

It has been widely documented that SQV has the ability to increase the occurrence of renal calculi (kidney stones), however, no renal toxicity has been attributed to SQV (58). The largest quantity of SQV released from SQV-MC was detected within the kidneys which is interesting, because typically less than 1% of SQV is excreted from the kidneys (51). The small percentage of renal excretion probably stems from the drastic first pass metabolism that occurs when SQV is dosed orally, meaning that SQV-MC could radically change the amount of non-metabolized SQV that reaches other organs. The quantity of SQV within the kidneys is meaningful, because HIV can cause nephropathy due to viral replication within the kidney (59). In fact, HIV has been detected within podocytes, parietal cells and renal tubular cells at high levels highlighting the ability of HIV to cause kidney damage and the subsequent importance of drug delivery to the kidney (60).

One aspect which was not investigated within this work is to boost SQV with RTV as is performed within the clinic (61, 62) which can lead to an increase in the orally administered area under the curve and C_{max} of SQV by over 50 and 22 fold, respectively (63). The potential to increase the serum concentrations and allow for passage through the blood brain barrier and testes using RTV could be coupled with the slow degrading SQV-MC, allowing for sustained delivery over a longer period of time than was achieved in the current study. A longer sustained release period from Ace-DEX-MC would lead to fewer required administrations and would cut down on the potential for non-adherence related complications. Additionally, if the serum concentrations are increased for a longer duration, it is likely that there will be a larger accumulation of SQV within the tissues (64) allowing for enhanced anti-viral activity throughout many of HIV's tissue reservoirs.

CONCLUSION

We have presented a novel, highly loaded delivery vehicle for the long acting release of saquinavir into systemic circulation to counteract adherence related resistance in the treatment of HIV. We show stable and relatively uniform fiber generation along with high encapsulation efficiencies of drug. Most interesting, is the ability to process our scaffolds into injectable MC and fine tune the release kinetics by changing the Ace-DEX carrier polymer's hydrolytic stability (cyclic acetal coverage) and total drug loading. These flexible options are unique to Ace-DEX and not possible with more ubiquitously used biodegradable polymers like PLGA. Finally, our work suggests that Ace-DEX-MC presents a platform by which other hydrophobic small molecule drugs can be loaded and released over time for enhanced pharmacologic effect.

ACKNOWLEDGMENTS AND DISCLOSURES

We would like to acknowledge the Chapel Hill Analytical and Nanofabrication Laboratory (CHANL) and Campus Microscopy and Imaging Facility (CMIF) for allowing us access to use the imaging equipment used within this manuscript. Additionally, we would like to acknowledge the University of North Carolina at Chapel Hill Center for AIDS Research (P30 AI50410).

REFERENCES

1. Organization WH. HIV/AIDS. Available from: http://www.who.int/hiv/en/.
2. Aids.gov. HIV Basics. Available from: https://www.aids.gov/.
3. Pauwels R. Aspects of successful drug discovery and development. Antivir Res. 2006;71(2–3):77–89.
4. Ledergerber B, Egger M, Erard V, Weber R, Hirschel B, Furrer H, *et al.* AIDS-related opportunistic illnesses occurring after initiation of potent antiretroviral therapy: the Swiss HIV Cohort Study. JAMA. 1999;282(23):2220–6.
5. Gardner EM, Burman WJ, Steiner JF, Anderson PL, Bangsberg DR. Antiretroviral medication adherence and the development of class-specific antiretroviral resistance. AIDS. 2009;23(9):1035–46.
6. von Hentig N, Nisius G, Lennemann T, Khaykin P, Stephan C, Babacan E, *et al.* Pharmacokinetics, safety and efficacy of saquinavir/ritonavir 1,000/100 mg twice daily as HIV type-1 therapy and transmission prophylaxis in pregnancy. Antivir Ther. 2008;13(8):1039–46.
7. Clavel F, Hance AJ. HIV drug resistance. N Engl J Med. 2004;350(10):1023–35.
8. Prevention CfDCa. Initiation of and adherence to treatment as prevention 2013.
9. Ananworanich J, Hirschel B, Sirivichayakul S, Ubolyam S, Jupimai T, Prasithsirikul W, *et al.* Absence of resistance mutations in antiretroviral-naive patients treated with ritonavir-boosted saquinavir. Antivir Ther. 2006;11(5):631–5.
10. Dickinson L, Boffito M, Khoo SH, Schutz M, Aarons LJ, Pozniak AL, *et al.* Pharmacokinetic analysis to assess forgiveness of boosted saquinavir regimens for missed or late dosing. J Antimicrob Chemother. 2008;62(1):161–7.
11. Kemp DE, Canan F, Goldstein BI, McIntyre RS. Long-acting risperidone: a review of its role in the treatment of bipolar disorder. Adv Ther. 2009;26(6):588–99.
12. Draper BH, Morroni C, Hoffman M, Smit J, Beksinska M, Hapgood J, *et al.* Depot medroxyprogesterone versus norethisterone oenanthate for long-acting progestogenic contraception. Cochrane Database Syst Rev. 2006;3:CD005214.
13. Nieschlag E, Buchter D, Von Eckardstein S, Abshagen K, Simoni M, Behre HM. Repeated intramuscular injections of testosterone undecanoate for substitution therapy in hypogonadal men. Clin Endocrinol. 1999;51(6):757–63.
14. McEvoy JP. Risks versus benefits of different types of long-acting injectable antipsychotics. J Clin Psychiatry. 2006;67(5):15–8.
15. Elzi L, Marzolini C, Furrer H, Ledergerber B, Cavassini M, Hirschel B, *et al.* Treatment modification in human immunodeficiency virus-infected individuals starting combination antiretroviral therapy between 2005 and 2008. Arch Intern Med. 2010;170(1):57–65.
16. Info A. Guidelines for the use of antiretroviral agents in HIV-1-Infected Adults and Adolescents. In.; 2015.
17. Robison LS, Westfall AO, Mugavero MJ, Kempf MC, Cole SR, Allison JJ, *et al.* Short-term discontinuation of HAART regimens more common in vulnerable patient populations. AIDS Res Hum Retrovir. 2008;24(11):1347–55.
18. Spreen WR, Margolis DA, Pottage Jr JC. Long-acting injectable antiretrovirals for HIV treatment and prevention. Curr Opin HIV AIDS. 2013;8(6):565–71.
19. Rabinow BE. Nanosuspensions in drug delivery. Nat Rev Drug Discov. 2004;3(9):785–96.
20. van't Klooster G, Hoeben E, Borghys H, Looszova A, Bouche MP, van Velsen F, *et al.* Pharmacokinetics and disposition of rilpivirine (TMC278) nanosuspension as a long-acting injectable antiretroviral formulation. Antimicrob Agents Chemother. 2010;54(5):2042–50.
21. Fung HW, Mikasa TJ, Vergara J, Sivananthan SJ, Guderian JA, Duthie MS, *et al.* Optimizing manufacturing and composition of a TLR4 nanosuspension: physicochemical stability and vaccine adjuvant activity. J Nanobiotechnol. 2013;11:43.
22. Kanthamneni N, Sharma S, Meenach SA, Billet B, Zhao JC, Bachelder EM, *et al.* Enhanced stability of horseradish peroxidase encapsulated in acetalated dextran microparticles stored outside cold chain conditions. Int J Pharm. 2012;431(1–2):101–10.
23. Kauffman KJ, Do C, Sharma S, Gallovic MD, Bachelder EM, Ainslie KM. Synthesis and characterization of acetalated dextran polymer and microparticles with ethanol as a degradation product. ACS Appl Mater Interfaces. 2012;4(8):4149–55.
24. Bachelder EM, Beaudette TT, Broaders KE, Dashe J, Frechet JM. Acetal-derivatized dextran: an acid-responsive biodegradable material for therapeutic applications. J Am Chem Soc. 2008;130(32):10494–5.
25. Borteh HM, Gallovic MD, Sharma S, Peine KJ, Miao S, Brackman DJ, *et al.* Electrospun acetalated dextran scaffolds for temporal release of therapeutics. Langmuir. 2013;29(25):7957–65.
26. Khorshidi S, Solouk A, Mirzadeh H, Mazinani S, Lagaron JM, Sharifi S, et al. A review of key challenges of electrospun scaffolds for tissue-engineering applications. J Tissue Eng Regen Med. 2015.
27. Passerini N, Craig DQ. An investigation into the effects of residual water on the glass transition temperature of polylactide microspheres using modulated temperature DSC. J Control Release: Off J Control Release Soc. 2001;73(1):111–5.
28. Singh L, Kumar V, Ratner BD. Generation of porous microcellular 85/15 poly (DL-lactide-co-glycolide) foams for biomedical applications. Biomaterials. 2004;25(13):2611–7.
29. Jung BH, Rezk NL, Bridges AS, Corbett AH, Kashuba AD. Simultaneous determination of 17 antiretroviral drugs in human plasma for quantitative analysis with liquid chromatography-tandem mass spectrometry. Biomed Chromatogr: BMC. 2007;21(10):1095–104.
30. Horn T. Transmitted HIV drug resistance on the rise in U.S. AIDSMEDS. 2012.
31. Jarvis WR, Jarvis AA, Chinn RY. National prevalence of methicillin-resistant Staphylococcus aureus in inpatients at United States health care facilities, 2010. Am J Infect Control. 2012;40(3):194–200.
32. Salamon H, Yamaguchi KD, Cirillo DM, Miotto P, Schito M, Posey J, *et al.* Integration of published information into a resistance-associated mutation database for Mycobacterium tuberculosis. J Infect Dis. 2015;211(2):S50–57.
33. Md. Fazley Elahi* WL, Guoping G, Khan F. Core-shell fibers for biomedical applications-a review. Bioeng Biomed Sci. 2013;3(1).
34. Duong AD, Sharma S, Peine KJ, Gupta G, Satoskar AR, Bachelder EM, *et al.* Electrospray encapsulation of toll-like receptor agonist resiquimod in polymer microparticles for the treatment of visceral leishmaniasis. Mol Pharm. 2013;10(3):1045–55.
35. Seif S, Franzen L, Windbergs M. Overcoming drug crystallization in electrospun fibers - Elucidating key parameters and developing strategies for drug delivery. Int J Pharm. 2015;478(1):390–7.

36. Serruys PW, Onuma Y, Dudek D, Smits PC, Koolen J, Chevalier B, *et al.* Evaluation of the second generation of a bioresorbable everolimus-eluting vascular scaffold for the treatment of de novo coronary artery stenosis: 12-month clinical and imaging outcomes. J Am Coll Cardiol. 2011;58(15):1578–88.
37. Yerragunta B, Jogala S, Chinnala KM, Aukunuru J. Development of a novel 3-month drug releasing risperidone microspheres. J Pharm Bioallied Sci. 2015;7(1):37–44.
38. Insert VP. Naltraxone for extended-release injectable suspension. 2015.
39. Reach V. Keeping the cold chain cold. 2014.
40. Perno CF, Newcomb FM, Davis DA, Aquaro S, Humphrey RW, Calio R, *et al.* Relative potency of protease inhibitors in monocytes/macrophages acutely and chronically infected with human immunodeficiency virus. J Infect Dis. 1998;178(2):413–22.
41. Davis DA, Read-Connole E, Pearson K, Fales HM, Newcomb FM, Moskovitz J, *et al.* Oxidative modifications of kynostatin-272, a potent human immunodeficiency virus type 1 protease inhibitor: potential mechanism for altered activity in monocytes/macrophages. Antimicrob Agents Chemother. 2002;46(2):402–8.
42. Mahajan SD, Roy I, Xu G, Yong KT, Ding H, Aalinkeel R, *et al.* Enhancing the delivery of anti retroviral drug "Saquinavir" across the blood brain barrier using nanoparticles. Curr HIV Res. 2010;8(5):396–404.
43. Prakashan N. Mechanical operations: fundamental principles and applications; 2007.
44. Champion JA, Mitragotri S. Role of target geometry in phagocytosis. Proc Natl Acad Sci U S A. 2006;103(13):4930–4.
45. Hrkach J. Targeted polymeric nanotherapeutics. In frontiers of engineering: reports on leading-edge engineering from the 2008 Symposium. 2008.
46. Fu Y, Kao WJ. Drug release kinetics and transport mechanisms of non-degradable and degradable polymeric delivery systems. Expert Opin Drug Deliv. 2010;7(4):429–44.
47. Ford J, Khoo SH, Back DJ. The intracellular pharmacology of antiretroviral protease inhibitors. J Antimicrob Chemother. 2004;54(6):982–90.
48. Crow BB, Borneman AF, Hawkins DL, Smith GM, Nelson KD. Evaluation of in vitro drug release, pH change, and molecular weight degradation of poly(L-lactic acid) and poly(D, L-lactide-co-glycolide) fibers. Tissue Eng. 2005;11(7–8):1077–84.
49. Lin YS, Nguyen C, Mendoza JL, Escandon E, Fei D, Meng YG, *et al.* Preclinical pharmacokinetics, interspecies scaling, and tissue distribution of a humanized monoclonal antibody against vascular endothelial growth factor. J Pharmacol Exp Ther. 1999;288(1):371–8.
50. Holladay JW, Dewey MJ, Michniak BB, Wiltshire H, Halberg DL, Weigl P, *et al.* Elevated alpha-1-acid glycoprotein reduces the volume of distribution and systemic clearance of saquinavir. Drug Metab Dispos: Biol Fate Chem. 2001;29(3):299–303.
51. AIDSinfo. Invirase Drug Database. Available from: https://aidsinfo.nih.gov/drugs/164/invirase/0/professional.
52. Gautam N, Roy U, Balkundi S, Puligujja P, Guo D, Smith N, *et al.* Preclinical pharmacokinetics and tissue distribution of long-acting nanoformulated antiretroviral therapy. Antimicrob Agents Chemother. 2013;57(7):3110–20.
53. Meeus J, Scurr DJ, Amssoms K, Wuyts K, Annaert P, Davies MC, *et al.* In vivo evaluation of different formulation strategies for sustained release injectables of a poorly soluble HIV protease inhibitor. J Control Release: Off J Control Release Soc. 2015;199:1–9.
54. Saksena NK, Wang B, Zhou L, Soedjono M, Ho YS, Conceicao V. HIV reservoirs in vivo and new strategies for possible eradication of HIV from the reservoir sites. HIV/AIDS. 2010;2:103–22.
55. Eagling VA, Wiltshire H, Whitcombe IW, Back DJ. CYP3A4-mediated hepatic metabolism of the HIV-1 protease inhibitor saquinavir in vitro. Xenobiotica; Fate Foreign Compounds Biol Syst. 2002;32(1):1–17.
56. Diaz LK, Murphy RL, Phair JP, Variakojis D. The AIDS autopsy spleen: a comparison of the pre-anti-retroviral and highly active anti-retroviral therapy eras. Modern Pathol: Off J U S Can Acad Pathol Inc. 2002;15(4):406–12.
57. Di Mascio M, Srinivasula S, Bhattacharjee A, Cheng L, Martiniova L, Herscovitch P, *et al.* Antiretroviral tissue kinetics: in vivo imaging using positron emission tomography. Antimicrob Agents Chemother. 2009;53(10):4086–95.
58. Daugas E, Rougier JP, Hill G. HAART-related nephropathies in HIV-infected patients. Kidney Int. 2005;67(2):393–403.
59. Weiner NJ, Goodman JW, Kimmel PL. The HIV-associated renal diseases: current insight into pathogenesis and treatment. Kidney Int. 2003;63(5):1618–31.
60. Tanji N, Ross MD, Tanji K, Bruggeman LA, Markowitz GS, Klotman PE, *et al.* Detection and localization of HIV-1 DNA in renal tissues by in situ polymerase chain reaction. Histol Histopathol. 2006;21(4):393–401.
61. Kempf DJ, Marsh KC, Kumar G, Rodrigues AD, Denissen JF, McDonald E, *et al.* Pharmacokinetic enhancement of inhibitors of the human immunodeficiency virus protease by coadministration with ritonavir. Antimicrob Agents Chemother. 1997;41(3):654–60.
62. Plosker GL, Scott LJ. Saquinavir: a review of its use in boosted regimens for treating HIV infection. Drugs. 2003;63(12):1299–324.
63. Buss N, Snell P, Bock J, Hsu A, Jorga K. Saquinavir and ritonavir pharmacokinetics following combined ritonavir and saquinavir (soft gelatin capsules) administration. Br J Clin Pharmacol. 2001;52(3):255–64.
64. Shahani K, Swaminathan SK, Freeman D, Blum A, Ma L, Panyam J. Injectable sustained release microparticles of curcumin: a new concept for cancer chemoprevention. Cancer Res. 2010;70(11):4443–52.